



## Research paper

## Controlled polymorphic transformation of continuously crystallized solid lipid nanoparticles in a microstructured device: A feasibility study

M. Schoenitz<sup>a,\*</sup>, S. Joseph<sup>b</sup>, A. Nitz<sup>a</sup>, H. Bunjes<sup>b</sup>, S. Scholl<sup>a</sup><sup>a</sup> Technische Universität Braunschweig, Institute for Chemical and Thermal Process Engineering (ICTV), Braunschweig, Germany<sup>b</sup> Technische Universität Braunschweig, Institute for Pharmaceutical Technology, Braunschweig, Germany

## ARTICLE INFO

## Article history:

Received 1 March 2013

Accepted in revised form 8 August 2013

Available online 20 August 2013

## Keywords:

SLN

Solid lipid nanoparticles

Continuous crystallization

Micro-heat exchanger

Drug delivery

Micro process engineering

Polymorphism

## ABSTRACT

The contribution describes the transfer from a batch to a micro-continuous process for the production of stable solid lipid nanoparticles as drug carrier systems. Solid lipid nanoparticles are commonly prepared batch-wise often resulting in poorly defined product qualities with regard to the polymorphic state of their lipid matrix. In order to obtain solid lipid nanoparticle dispersions that meet the requirements for an acceptable pharmaceutical product, the manufacture of reproducible product qualities preferably containing the stable crystal form of the respective matrix lipid is necessary. These requests are addressed by the continuous preparation process of solid lipid nanoparticles. A four step feasibility study for the standardized evaluation whether or not a colloidal lipid dispersion is suitable for continuous crystallization of the particles resulting in stable crystal forms is presented. The process is based on the continuous crystallization and subsequent thermal treatment of differently stabilized, tripalmitin-based nanoparticle formulations in microstructured devices. The successful production of the stable crystal form by means of a continuous process chain is shown for a dispersion stabilized with a blend of hydrogenated soybean lecithin and sodium glycocholate.

© 2013 Elsevier B.V. All rights reserved.

## 1. Introduction

Moving from batch to micro-continuous processes is based on the multi-scale approach described by Bayer et al. [1] and can lead to shorter process development resulting in a shorter time-to-market [2]. A general comparison between micro-continuous and batch plants can be found in [3]. Specifically for pharmaceutical applications, the manufacture of products stable over the whole shelf life is imperative. Pharmaceutical products consisting of triglycerides can occur in different metastable and stable crystal modifications, leading to challenging process development with regard to the production of stable crystal forms. A concept for the continuous crystallization with subsequent thermal treatment to obtain the stable crystal form in a continuous process chain is described in the following for dispersions of solid triglyceride nanoparticles. Additionally, a screening method is presented, which can identify promising formulations with regard to continuous processability.

## 1.1. Solid lipid nanoparticles

First approached by Speiser in 1986 [4] and finally developed by different groups in the beginning of the 1990s [5–7], solid lipid nanoparticles (SLN) still offer a high innovative potential for pharmaceutical, cosmetic and food applications [8–10]. SLN are composed of an emulsifier-stabilized lipid matrix with a particle diameter of 100–500 nm. These particles can be used as carriers for lipophilic active ingredients. For instance, poorly water soluble drugs suffering from a poor oral bioavailability can be incorporated into SLN formulations to improve their pharmaceutical performance. Moreover, the particles are interesting as carriers for the parenteral delivery of lipophilic drugs [11–14]. In particular with regard to parenteral administration, the lipidic nature of the matrix components is often regarded as an advantage, in particular compared to polymeric carrier systems [15]. Also the food industry discovered SLN as a powerful approach to formulate bioactive compounds such as vitamins, carotenoids or omega-3 fatty acids to create functional food [16–18].

Different preparation procedures for SLN have been evaluated [13]. Currently, the most promising in regard to industrial production is the high-pressure homogenization of a melted lipid phase in an emulsifier-containing aqueous phase and subsequent cooling to crystallize the particles [12]. SLN can occur in different crystalline modifications, reflecting the polymorphism of the matrix lipid

\* Corresponding author. Technische Universität Braunschweig, Institute for Chemical and Thermal Process Engineering (ICTV), Langer Kamp 7, D-38106 Braunschweig, Germany. Tel.: +49 (0)531 391 2781.

E-mail addresses: [m.schoenitz@tu-braunschweig.de](mailto:m.schoenitz@tu-braunschweig.de) (M. Schoenitz), [heike.bunjes@tu-braunschweig.de](mailto:heike.bunjes@tu-braunschweig.de) (H. Bunjes).

involved. The polymorphism of triglycerides, which are often used as matrix lipids in SLN, depends on the conditions during crystallization and subsequent procedures. Rapid cooling favors the formation of the metastable  $\alpha$ -modification, which monotropically transforms into the stable  $\beta$ -modification in a time- and temperature-dependent manner, sometimes via the metastable  $\beta'$ -form [19]. Short-chain triglycerides perform this transition more rapidly than long-chain triglycerides; some mixed-chain triglycerides tend to remain in a metastable form even after extended periods of storage [20,21]. The batch-wise crystallization process commonly used in the preparation of SLN typically involves low cooling rates frequently yielding mixtures of SLN in the  $\alpha$ - and  $\beta$ -modification [22]. For industrial purposes, crystals in the stable polymorphic form are preferred, as products that change their properties during shelf life are unacceptable for almost any type of application. Polymorphic transformation of triglyceride nanoparticles might, for example, result in alterations of the drug distribution within the formulation or formulation viscosity [12,23,24].

However, for many formulations, a direct, complete crystallization of the particles into the stable  $\beta$ -modification is not possible. The stable state of such formulations may only be reached via the primary metastable  $\alpha$ -modification and potentially the intermediate metastable  $\beta'$ -modification. Therefore, this work focuses on the establishment of a continuous, precisely controlled process that allows the formation of triglyceride SLN in the stable  $\beta$ -form directly after crystallization. The process is based on the crystallization of the particles into the metastable  $\alpha$ -form or into a reproducible mixture of particles in the  $\alpha$ - and  $\beta$ -form in a micro-heat exchanger and subsequent continuous thermal treatment in order to achieve the transformation into the stable  $\beta$ -form.

### 1.2. Continuous crystallization of SLN

First efforts toward a continuous crystallization of SLN in a micro-heat exchanger after high-pressure melt homogenization have been reported by Jasch et al. [25]. The major benefits of continuous SLN crystallization compared to batch processing originate from superior process control possibilities resulting in well-defined and highly reproducible product properties as well as an easier scale-up to industrial scale [2]. Specifically, the advantages in process control are of high interest, because spatial and time distribution of relevant process parameters can lead to different crystal modifications and thus to a broad distribution of product qualities. For the same production capacity, product holdup in the equipment is typically much lower for continuous compared to batch processing. This is of special relevance for pharmaceutical applications where product availability is a crucial aspect in early stages of process development. Furthermore, the continuous approach allows the preparation of well-defined lipid dispersions in a shorter time compared to batch-wise processing and is thus a potential tool for screening purposes. With continuous crystallization in a micro-heat exchanger, high cooling rates with a very narrow residence time distribution could be realized. For the triglyceride formulations under investigation, particles in the metastable  $\alpha$ -modification were obtained [25].

### 1.3. Thermal treatment to obtain the stable $\beta$ -form

In order to obtain stable crystal modifications of triglycerides in SLN dispersions after continuous processing, it is necessary to establish the required conditions for the  $\alpha$  to  $\beta$  transition. For some bulk materials, such conditions can be taken from the literature. Kellens and Reynaers obtained the  $\beta$ -form of bulk tristearin by recrystallization from the  $\alpha$ -form in a thermal treatment step at 66 °C (i.e., a temperature between the melting point of the  $\alpha$ - and the  $\beta$ -modification) for 180 min [21]. For the  $\alpha$  to  $\beta$

transformation of tripalmitin, 90 min at 42 °C (a temperature slightly below the melting point of the  $\alpha$ -modification) was found sufficient [24,26]. The crystallization behavior and kinetics of polymorphic transition of colloiddally dispersed triglycerides differ, however, distinctly from those of the bulk material. The particles usually crystallize at much higher supercooling and the polymorphic transitions proceed more rapidly than in the bulk material [27,28]. Also the melting temperatures may be altered as a result of the small dimensions of the nanoparticles [27,29]. Thus, transformation conditions reported for the bulk materials cannot be simply transferred to the processing of corresponding nanoparticle dispersions. Moreover, not only the conditions of thermal treatment (such as temperature and residence time) but also the composition of the dispersion, in particular the stabilizers, have an effect on the polymorphic transition rate [30–32]. Hence, suitable parameters for the transformation into the stable crystal form have to be identified for each SLN formulation of interest. This study introduces a strategy to find useful process parameters for the transformation and describes a strategy for the identification and the realization in a continuous micro-process chain resulting in a stable product for a tripalmitin formulation representing a well-characterized model system.

## 2. Materials and methods

### 2.1. Materials

Tripalmitin (Dynasan<sup>®</sup> 116, purity 97%, Sasol Germany GmbH, Hamburg, Germany), poly(vinyl alcohol) (PVA) (Mowiol 3-83, Kuraray Europe GmbH, Frankfurt/Main, Germany), hydrogenated soybean lecithin (S100-3) (containing  $\geq 94\%$  phosphatidylcholine, Lipoid S100-3, Lipoid KG, Ludwigshafen, Germany), sodium glycocholate hydrate (SGC) ( $\geq 97\%$ ), Sigma-Aldrich Chemie GmbH, Steinheim, Germany), glycerol 85%, and thimerosal (both supplied from Caesar und Loretz GmbH, Hilden, Germany) were used as received. Water was prepared by double distillation.

### 2.2. Methods

#### 2.2.1. Composition and preparation of dispersions

Two different dispersions (Table 1) were used in the experiments.

The matrix lipid and the aqueous phase containing emulsifiers, glycerol, and thimerosal (batch size 1 L) were heated to 85 °C with a temperature controlled magnetic stirrer (IKA<sup>®</sup> RCT basic, IKA<sup>®</sup>-Werke GmbH & Co. KG, Staufen, Germany) and then predispersed with an ultraturrax at 19000 rpm for 3 min (Ultra-Turrax<sup>®</sup> IKA T18, IKA<sup>®</sup>-Werke GmbH & Co. KG, Staufen, Germany). The pre-emulsions were transferred to a Niro Soavi homogenizer (Panda 3649, Parma, Italy) equipped with a thermostatic water bath (Haake D1, Thermo Haake GmbH, Karlsruhe, Germany) and were emulsified for 90 min (equal to 30 cycles) at 85 °C at a pressure of 300–330 bar. Crystallization was induced via stirring in an ice-water bath. The evaporated water from the particle dispersion

**Table 1**  
Compositions of SLN dispersions.

	PVA-stabilized (wt%)	S100-3/SGC-stabilized (wt%)
Tripalmitin	15	15
SGC		0.9
Soybean lecithin		3.6
Poly(vinyl alcohol)	7.5	
Glycerol 85%	2.13	2.20
Thimerosal	0.01	0.01
Aqua bidest.	ad 100	ad 100

was replenished with bidistilled water at the end of the process. Dispersions were stored in a refrigerator.

### 2.2.2. Photon Correlation Spectroscopy (PCS)

The mean particle size was determined by PCS at 25 °C (Zetasizer-Nano-ZS, Malvern Instruments, Herrenberg, Germany) directly after sampling. The dispersions were diluted with purified, particle-free water (4 M $\Omega$ /cm) obtained from a Purelab UHQ system (ELGA LabWater, Celle, Germany) to an appropriate scattering intensity. The measurements were performed with four runs, each 300 s, after an equilibration time of 120 s at 25 °C. The results (mean of the four measurements) are given as the particle diameter (z-average) and the polydispersity index (PDI), quantifying the width of the particle size distribution.

### 2.2.3. Differential Scanning Calorimetry (DSC)

The crystalline modification of the lipid particles was analyzed by DSC (DSC 1 equipped with an autosampler, Mettler Toledo, Greifensee, Switzerland). For measurements, approximately 8  $\mu$ L of the dispersions was weighed into aluminum pans (K-YSSC000C008, Thass GmbH, Friedberg, Germany) and cold welded. The samples were kept at 5 °C for 1 min, heated to 85 °C with 10 K min<sup>-1</sup>, and held at that temperature for 3 min. The normalized heat flux (W g<sup>-1</sup>) was recorded against the sample temperature.

### 2.2.4. Batch crystallization

To ensure that all incubation experiments were carried out with identical starting conditions, standardized batch crystallization was performed before these experiments were run. The stored dispersions were heated to 85 °C under stirring in an oil bath and held at that temperature for 15 min to ensure complete melting of all crystals. Afterward, crystallization was induced by putting the samples in an ice bath and cooling down to 5 °C.

### 2.2.5. $\alpha$ to $\beta$ transition temperature screening

The temperature-dependent  $\alpha$  to  $\beta$  transition behavior was determined in a series of 24 h experiments at different temperatures ranging from 37 °C to 50 °C. Vials with 2 mL dispersion each were held at the respective temperature in a thermostat (Huber ministat cc-230, Offenburg, Germany) with double sampling every 2 h. The samples were stored at refrigerator temperature (5 °C) for a maximum of 3 days before they were investigated by DSC. PCS measurements were performed directly after sampling.

### 2.2.6. Continuous melt crystallization

Continuous melt crystallization was performed in a micro-heat exchanger (Karlsruhe Institute of Technology) consisting of two polymer half shells and a stainless steel foil with integrated micro-channels on both sides (Fig. 1). The foil had eight parallel rectangular channels with a cross-section of 400  $\times$  400  $\mu$ m and 190 mm length each. The basic process concept was investigated by Jasch et al. [25] and the experimental setup is shown in Fig. 2.

Prior to feeding product to the equipment, thermal equilibrium in the setup was established. Water with a temperature of 80 °C was circulated from a reservoir through the dispersion feed line, the micro-heat exchanger and back to the reservoir (Fig. 2). When thermal equilibrium was reached, three-way valves V1 and V2 were switched. Thus, the dispersion, previously heated to 85 °C to melt all particles and stored in a temperature controlled stirred vessel, entered the micro-heat exchanger with a temperature of 70 °C and was cooled down to 5 °C. Sampled dispersions were stored in an ice bath for a maximum of 1 day for further investigations. The connections between the different micro-devices were realized with PTFE tubes with inner diameters of 1/16". The micro-annular gear pump P1 (mzr-7205 by HNP Mikrosysteme GmbH, Parchim, Germany) was able to set volumetric flow rates of emulsion from 2 to 40 mL min<sup>-1</sup>. Cooling rates were calculated based on temperature differences between the entrance ( $T_{in}$ ) and the exit ( $T_{out}$ ) of the micro-heat exchanger combined with the average residence time ( $\tau_{\mu ch}$ ) in the channels of the micro-heat exchanger, see Eq. (1). The residence time was calculated with the micro-channels volume ( $V_{\mu ch}$ ) and the volumetric flow rate ( $\dot{V}$ ).

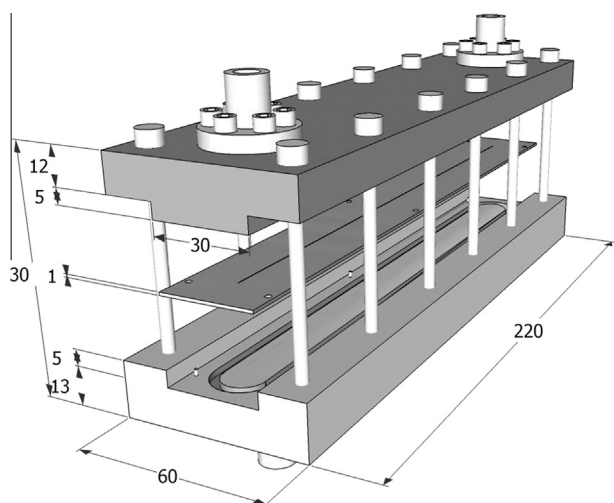


Fig. 1. Scheme of the micro-heat exchanger (dimensions in mm).

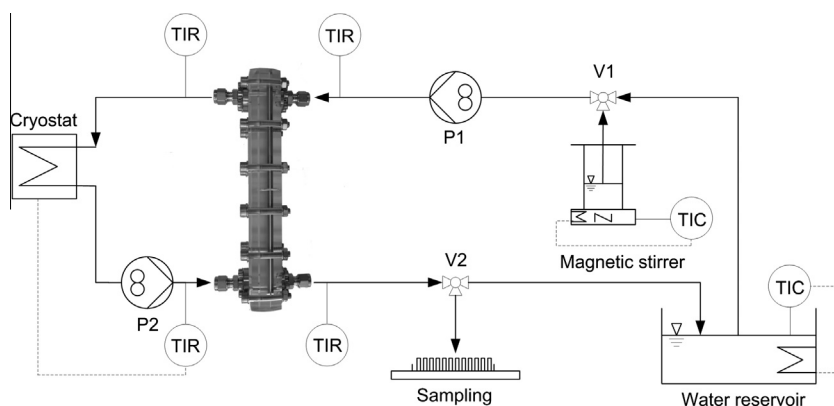


Fig. 2. Experimental setup for continuous melt crystallization of SLN in a micro-heat exchanger, modified from [25].

$$\text{Cooling rate} = \frac{(T_{\text{in}} - T_{\text{out}})}{\tau_{\mu\text{ch}}} = \frac{(T_{\text{in}} - T_{\text{out}}) \cdot \dot{V}}{V_{\mu\text{ch}}} \quad (1)$$

### 2.2.7. Controlled continuous $\alpha$ to $\beta$ transformation

Continuous  $\alpha$  to  $\beta$  transformation experiments were realized in a thermal residence time section (Fig. 3). The thermal residence time section had a length of 10 m (PTFE tube with inner diameter of 1/16"), which was placed in a thermostat with constant temperature (42 °C). The above mentioned micro-annular gear pump was used to realize different residence times of 30 and 60 min by adjusting the flow rate. The residence time  $\tau_{\text{rts}}$  in the residence time section was calculated based on the inner volume  $V_{\text{rts}}$  of the PTFE tube and the volumetric flow rate  $V$ :

$$\tau_{\text{rts}} = \frac{V_{\text{rts}}}{V} = \frac{\pi d_i^2 L}{4V} \quad (2)$$

## 3. Results and discussion

### 3.1. Determining crystal fractions

The enthalpies of the melting ( $E_\alpha$  and  $E_\beta$ ) and recrystallization ( $E_{\beta,\text{re}}$ ) events during the DSC heating run of the suspensions containing 15% tripalmitin were used to determine the fraction of triglyceride in the  $\alpha$ - and  $\beta$ -form ( $a_\alpha$  and  $a_\beta$ ). To determine the melting enthalpies of particles in the  $\alpha$ - and  $\beta$ -form as a reference, DSC measurements with samples that had completely been transformed into the  $\alpha$ - or  $\beta$ -form, respectively, were performed.  $\alpha$ -form samples were obtained within the DSC device by melting of the sample and subsequent cooling to recrystallize the particles into the  $\alpha$ -form.  $\beta$ -form samples were obtained by 10 days of storage at 35 °C. The subsequent DSC measurements were performed in triplicate and under the assumption that the samples contained 100%  $\alpha$ - or  $\beta$ -form, respectively.

As demonstrated in Fig. 4, the melting enthalpy of  $\alpha$ -form nanoparticles was  $E_\alpha = 14.42 \pm 0.37 \text{ J g}^{-1}$ . This value is considerably lower than that obtained for nanoparticles in the  $\beta$ -form with  $E_\beta = 23.14 \pm 0.32 \text{ J g}^{-1}$ . Thus, a correction factor of  $E_\alpha/E_\beta = 0.62$  was used for  $\beta$ -form melting enthalpies for the calculation of  $\alpha$ - and  $\beta$ -form fractions with Eq. (3).

For tripalmitin bulk material, melting enthalpies of  $E_\alpha = 116\text{--}128 \text{ J g}^{-1}$  and  $E_\beta = 202\text{--}205 \text{ J g}^{-1}$  have been reported [19], which give a similar value of  $E_\alpha/E_\beta = 0.60$  as found for our particles (0.62). The literature data would, however, result in  $E_\alpha = 17\text{--}19 \text{ J g}^{-1}$  and  $E_\beta = 30\text{--}31 \text{ J g}^{-1}$  for a sample containing 15% tripalmitin. Apparently, the sample under investigation here contained less than 15% tripalmitin probably due to dilution processes during preparation. As, however, only relative values were considered in our studies, such effects should not affect the overall results.

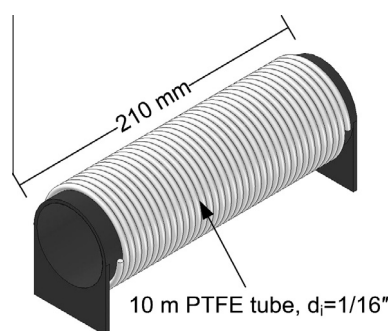


Fig. 3. Thermal residence time device for the continuous  $\alpha$  to  $\beta$  transition.

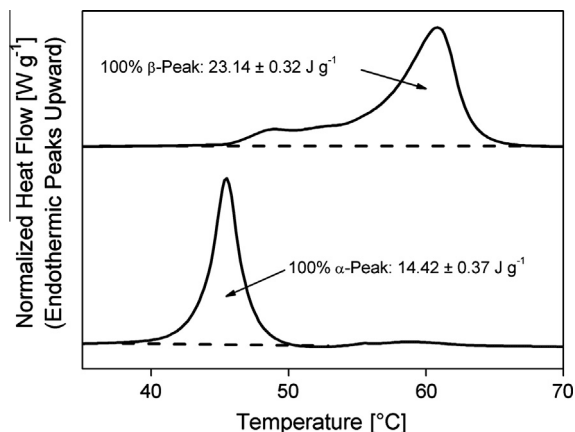


Fig. 4. DSC heating curves of PVA-stabilized dispersion after thermal treatment in order to achieve 100% of the  $\alpha$ - and  $\beta$ -form.

When determining the melting enthalpy for the  $\beta$ -form from the DSC curves, it has to be taken into account that recrystallization of nanoparticles into the  $\beta$ -form may occur during the DSC measurements.  $\beta$ -form recrystallization is indicated by an exothermic crystallization event directly after the  $\alpha$ -form melting endotherm (see for example 0 h curve in Fig. 12). This has to be considered by a correction of  $E_\beta$  by the  $\beta$ -form recrystallization enthalpy  $E_{\beta,\text{re}}$ . Unfortunately, the quantitative evaluation of some DSC curves showed uncertainties due to baseline irregularities. The values obtained should thus be regarded as approximations.

$$a_\beta = \frac{0.62(E_\beta - E_{\beta,\text{re}})}{E_\alpha + 0.62(E_\beta - E_{\beta,\text{re}})}; \quad a_\alpha = \frac{E_\alpha}{E_\alpha + 0.62(E_\beta - E_{\beta,\text{re}})} \quad (3)$$

More detailed information regarding Eq. (3) is given in the [Supplementary data](#).

### 3.2. $\alpha$ to $\beta$ Transformation during thermal treatment

Fig. 5 shows DSC melting curves for the PVA-stabilized formulation obtained directly after batch crystallization (A) or after 24 h of storage at 37 °C (B). An endothermic response indicates the melting of the  $\alpha$ -modification at about 45–46 °C and at approximately 60 °C for the  $\beta$ -modification. Crystallization with high cooling rates, for example in the micro heat exchanger, leads to the metastable  $\alpha$ -form in the PVA stabilized particles. Thermal treatment at 37 °C resulted in the transformation of a large portion of

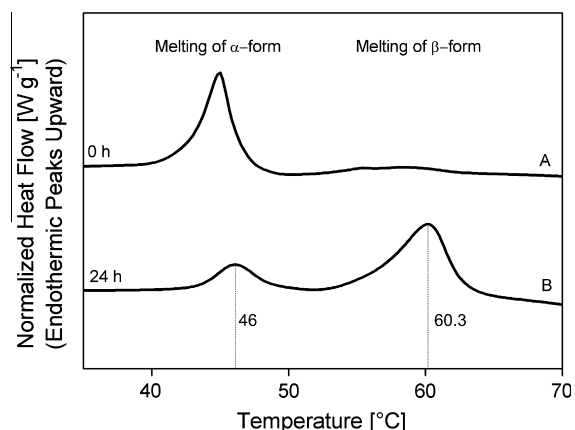


Fig. 5. DSC heating curves of a PVA-stabilized dispersion directly after crystallization and after storage for 24 h at 37 °C.

$\alpha$ -modification into the  $\beta$ -form. However, a significant amount of  $\alpha$ -modification remained, as indicated by the respective melting peak in curve B. Consequently, thermal treatment at 37 °C for 24 h was not sufficient to transform the initial formulation completely into the  $\beta$ -modification.

In general, the degree of transformation depends on the composition of the formulation and the process conditions in the transformation stage. Based on plant holdup, minimum flow rate and Reynolds number, respectively, as well as pressure drop considerations, a maximum residence time of 4 h is assumed to be realistic in a continuous micro-device process chain. Thus, further investigations were performed aiming at the identification of SLN formulations fitting into this processing scheme.

In the following, a four step feasibility study for the decision whether or not a SLN dispersion is suitable for continuous crystallization in a micro-heat exchanger with following continuous transformation to the stable  $\beta$ -modification is presented. The study is based on the polymorphic transition kinetics of the respective SLN composition.

### 3.3. Four step feasibility study

The feasibility study consists of four steps:

- (i) characterization of the SLN dispersion concerning the melting points of involved crystal modifications,
- (ii) determination of the maximum temperature which can be used for a thermally induced polymorphic transformation into the stable  $\beta$ -modification without melting the existing metastable  $\alpha$ -form,
- (iii) evaluation of the  $\alpha$  to  $\beta$  transition kinetics,
- (iv) final decision, if the continuous polymorphic transition to the stable crystal modification is possible in the defined timescale of 4 h.

The application of the four step feasibility study for the PVA-stabilized formulation is shown in the following.

#### 3.3.1. First step: Characterization of melting behavior of initial SLN formulation

To perform the polymorphic transformation by thermal treatment, a sufficient temperature range with respect to the distance of the crystal melting points of the involved species is needed. The melting points of the lipid particles representing different crystal modifications were determined from DSC measurements (Fig. 5). The sample, produced via batch crystallization, was stored for 24 h at a temperature 5 K below the melting point of the  $\alpha$ -modification of the corresponding lipid bulk material. After that time, the DSC curve displayed clear melting endotherms for the  $\alpha$ - as well as the  $\beta$ -form of tripalmitin at 46 °C and 60 °C, respectively. Peak temperatures were used as approximated melting temperatures of the regarding crystal form.

#### 3.3.2. Second step: Determining the maximum applicable temperature for the thermally induced $\alpha$ to $\beta$ transformation

Following melt homogenization, stable  $\beta$ -modification tripalmitin particles may only be obtained through polymorphic transformation from the metastable  $\alpha$ -form and not directly from the melt. For the transformation step, it is crucial to know the maximum temperature under which the rearrangement of the  $\alpha$ -polymorph to the  $\beta$ -form can be induced without melting the  $\alpha$ -form itself. Therefore, the freshly crystallized SLN were stored for 24 h at different temperatures, ranging from 37 to 50 °C, and were subsequently investigated by DSC (Fig. 6). The highest investigated temperatures (46 and 50 °C) were chosen at or above the melting point of the  $\alpha$ -polymorph to get detailed information over the

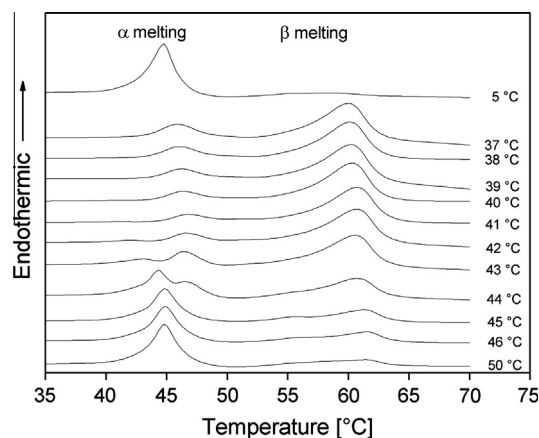


Fig. 6. DSC curves of PVA-stabilized tripalmitin dispersions stored for 24 h at the specified temperatures.

whole temperature range, clearly below, around, and above the  $\alpha$ -form melting point, respectively. 50 °C is 4 K above the  $\alpha$ -form melting point, and thus, this sample was presumably liquid during the experiment. The resulting 13% of the  $\beta$ -form were probably formed during tempering or post-processing (crystallization in refrigerator, storage time until DSC measurements).

With increasing storage temperature, a changeover from  $\alpha$ - to  $\beta$ -endotherm can be observed. Interestingly, the  $\alpha$ -modification seems to melt at two different temperatures in these samples. For example, the sample stored at 5 °C displays an endotherm of the  $\alpha$ -modification with a peak temperature around 44–45 °C, whereas the peak of the  $\alpha$ -endotherms is observed around 46 °C for samples stored at 37–40 °C. Samples stored at 43 °C and 44 °C display a double endotherm for the  $\alpha$ -form. Tentatively, the occurrence of two maxima in the transition region of the  $\alpha$ -modification might point to the presence of a nonlamellar and the common, lamellar  $\alpha$ -modification that have previously been observed by X-ray diffraction in similar triglyceride nanoparticles [30,32]. In this study, different types of  $\alpha$ -form (if present) were assumed to have the same melting enthalpy since no significant deviation from the generally occurring  $E_{\alpha}/E_{\beta}$  ratio was observed. The slight increase in  $\alpha$ -melting temperature in “older” samples (Fig. 9) might be due to aging processes. These phenomena are, however, poorly understood and call for further, more detailed investigations in the future.

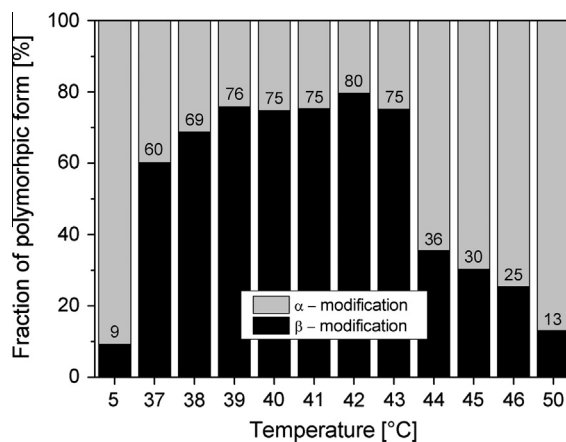


Fig. 7. Fraction of  $\alpha$ - and  $\beta$ -modification of PVA-stabilized particles after storage of 24 h at different temperatures. Numbers above the black bars give the fraction of  $\beta$ -form.

The DSC melting curves for samples stored at 45, 46, and 50 °C display an additional endotherm at 55 °C, which might indicate the presence of the  $\beta'$ -form. In an earlier study, Schaal observed the PVA-promoted formation of  $\beta'$ -crystals for trilaurin suspensions [33].

Fig. 7 shows the fraction of PVA-stabilized particles in the  $\alpha$ - and  $\beta$ -polymorph calculated from these DSC curves according to Eq. (3). The fraction of  $\beta$  modification increases with temperature until it reaches a plateau of around 75% from 39 °C to 43 °C. At higher temperatures, it decreases significantly. This indicates that a significant fraction of particles has melted at these temperatures and recrystallized into the  $\alpha$ -modification upon subsequent cooling.

The z-average and PDI values of these dispersions are given in Fig. 8. The z-average increases from about 150 nm after storage at 5 °C (control sample) up to a maximum of about 190 nm after storage at 40 °C. At higher temperatures, the z-average value tends to decrease again, particularly at storage temperatures above 45 °C. At the maximum investigated temperature of 50 °C, the initial value is nearly re-obtained with about 160 nm. The temperature dependence of the z-average value thus roughly follows the same pattern as the temperature-dependent evolution of the  $\beta$ -form fraction (Fig. 7). As particles in the  $\beta$ -modification are usually more anisometric (block- or platelet-like) than those in the  $\alpha$ -modification (spheroidal) and since anisometric particles tend to yield higher z-average values than corresponding spherical ones, these alterations in z-average diameter might reflect changes in particle shape during the polymorphic transformation [30,32,34,35].

In conclusion for step two, the maximum temperature for continuous polymorphic transformation of PVA-stabilized tripalmitin particles is 42 °C, as the polymorphic transformation from the  $\alpha$ -modification to the  $\beta$ -form proceeds without pronounced melting of particles in the  $\alpha$ -form. Distinctly higher temperatures would result in partial melting of the  $\alpha$ -modification with subsequent recrystallization (after cooling) to the  $\alpha$ -modification.

### 3.3.3. Third step: Determining the kinetics of polymorphic transition

The third step addresses the kinetics of polymorphic transition of  $\alpha$ - to  $\beta$ -modification in SLN. Freshly recrystallized particles were incubated at a transformation temperature of 42 °C with sampling every 2 h. The DSC melting curves of the corresponding samples (Fig. 9) show the increase in the amount of  $\beta$ -modification with time. As mentioned in step two, different  $\alpha$ -form melting temperatures were observed.

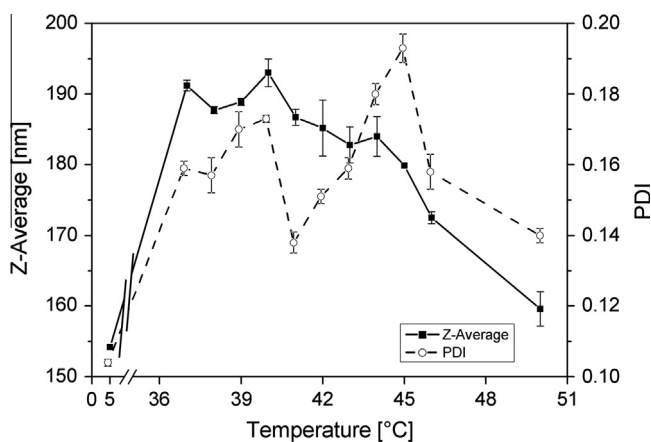


Fig. 8. z-Average and PDI of PVA-stabilized particles stored for 24 h at different temperatures (two independent samples). The single data points are connected for better visualization.

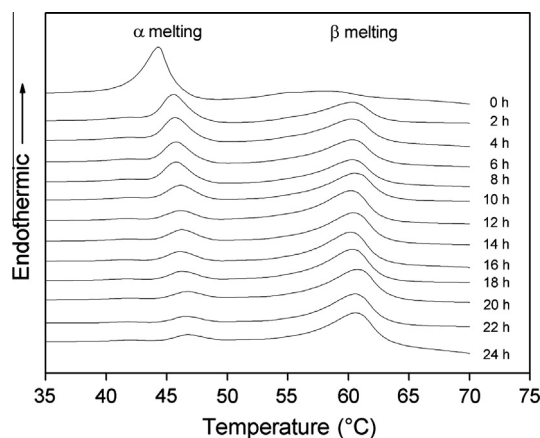


Fig. 9. DSC curves of PVA-stabilized nanoparticles showing the  $\alpha$  to  $\beta$  transition kinetics at 42 °C.

The quantitative evaluation of these DSC melting curves yields the increase in the fraction of  $\beta$ -modification over time at the storage temperature of 42 °C (Fig. 10). After 24 h, about 80% of the particles had transformed into the  $\beta$ -form. This transformation was accompanied by a steady increase in z-average particle size (Fig. 11), in agreement with the observations in step two. Although the PDI increased slightly (mainly during the first hours of incubation), it remained below 0.2 in all cases.

The experimental data points for the  $\alpha$  to  $\beta$  transformation kinetics (Fig. 10) were fitted using a generalized rate law according to Eq. (4) based on the fraction  $a_\alpha$  of the  $\alpha$ -polymorph:

$$-\frac{da_\alpha}{dt} = ka_\alpha^n \quad (4)$$

The dashed line in Fig. 10 is obtained by transforming Eq. (4) into Eq. (5) with a pseudo-order of  $n = 2.37$  and a reaction rate constant of  $k = 3.36 \times 10^{-4} \text{ h}^{-1}$ :

$$a_\beta = 1 - a_\alpha = 1 - \frac{1}{\left[ \frac{1}{a_{\alpha,0}^{n-1}} + (n-1)kt \right]^{-1}} \quad (5)$$

Based on the results of the experiments performed in the first three steps, the suitability for continuous processing of the regarding formulation is evaluated in the fourth step.

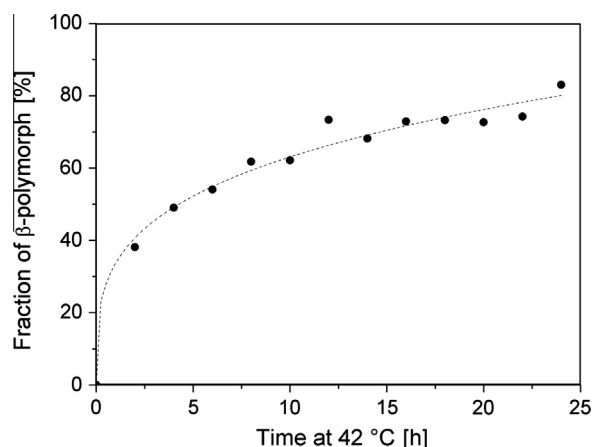


Fig. 10. Fraction of  $\beta$ -modification in PVA-stabilized particles over time at a storage temperature of 42 °C.

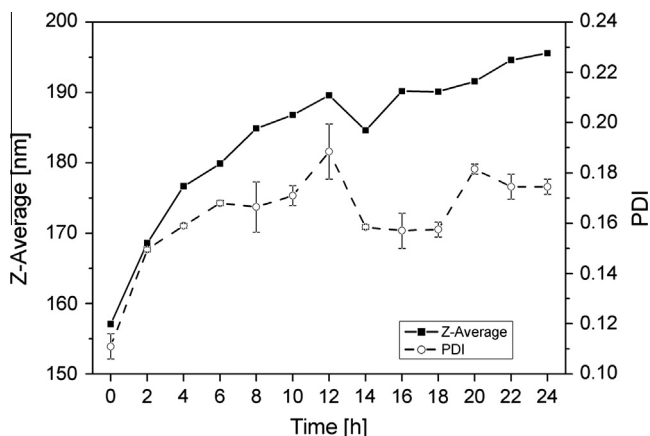


Fig. 11. z-Average and PDI of PVA-stabilized tripalmitin nanoparticles during the  $\alpha$  to  $\beta$  transition at 42 °C (two independent samples).

### 3.3.4. Fourth step: Decision if the SLN formulation is suitable for continuous processing

The fourth step deals with the decision whether the SLN composition is suitable for the polymorphic transition in a continuous process chain with a maximum transition time of 4 h or not. For the PVA-stabilized tripalmitin system under investigation, Fig. 10 reveals an incomplete polymorphic transition from the  $\alpha$ - to the  $\beta$ -form even after 24 h. In the defined 4 h time frame for the continuous crystallization, about 50% of the SLN had transformed into the stable  $\beta$ -modification. Thus, the required 100% of the stable  $\beta$ -form cannot be realized for this formulation in a continuous process chain under the given boundary conditions.

### 3.4. Application of the four step screening method for formulation and process development

Besides process parameters for the thermal treatment, mainly temperature and residence time, the composition of lipid dispersions – for example, the stabilizers – exerts a strong influence on the polymorphic transition kinetics. To investigate the influence of the compounds of the lipid dispersion on the suitability for continuous crystallization with subsequent polymorphic transition, a second tripalmitin dispersion stabilized by a mixture of sodium glycocholate (SGC) and hydrogenated soybean lecithin (S100-3)

was investigated. This emulsifier system accelerates the  $\alpha$  to  $\beta$  transition as compared to stabilization with PVA [31,32]. Furthermore, the suitability of the evaluated devices/methods for different dispersions with regard to their physical stability after thermal treatment was under investigation. The maximum temperature of 42 °C for the  $\alpha$ -to- $\beta$  transformation, found for the PVA-stabilized formulation, was used also for the S100-3/SGC-stabilized dispersion. Experimental investigations of step three were carried out for the sodium glycocholate and hydrogenated soybean lecithin-stabilized dispersion as described above.

As depicted in Fig. 12, the DSC curve of the S100-3/SGC-stabilized tripalmitin dispersion contained melting events for the  $\alpha$ - and  $\beta$ -form after batch crystallization (0 h). Percentage values are not given here to avoid ambiguities, because the hydrogenated soybean lecithin itself undergoes a thermal transition within the  $\beta$ -form melting event. Already after 0.5 h of storage at 42 °C, a complete  $\alpha$  to  $\beta$  transition could be observed, and the curve did not change much upon further storage up to 24 h. These results confirm the assumption of a more rapid polymorphic transformation in S100-3/SGC- than in PVA-stabilized tripalmitin dispersions. During the first half hour of storage at 42 °C, the particle size increased from about 198 nm to 238 nm and the PDI from 0.09 to 0.2. Starting at a storage time of 0.5 h, the z-average and PDI decreased to a constant value of 223 nm and 0.16. Thus, there was no indication for physical destabilization of the particles due to thermal treatment.

The comparison of PVA- and S100-3/SGC-stabilized particles reveals that for continuous processing to stable polymorphic forms, formulations with fast  $\alpha$  to  $\beta$  transition kinetics are beneficial.

#### 3.4.1. General processability in a continuous set-up

As demonstrated above with batch processes, S100-3/SGC-stabilized tripalmitin dispersions display comparatively fast transition kinetics that allow continuous processing into the stable  $\beta$ -modification within the defined 4 h time frame. For this formulation, a continuous process chain consisting of melt crystallization in a micro-heat exchanger followed by thermal treatment in a residence time device was established (Fig. 3). The continuous crystallization was realized with a cooling rate of 40 K s<sup>-1</sup> in the micro-heat exchanger followed by a subsequent thermal treatment in the residence time section for 1 h at 42 °C. The corresponding DSC melting curves are shown in Fig. 13.

Continuous crystallization at this high cooling rate of 40 K s<sup>-1</sup> leads to a significant  $\alpha$ -form melting event in the resulting suspension. A 100%  $\beta$ -form containing dispersion could be achieved with a

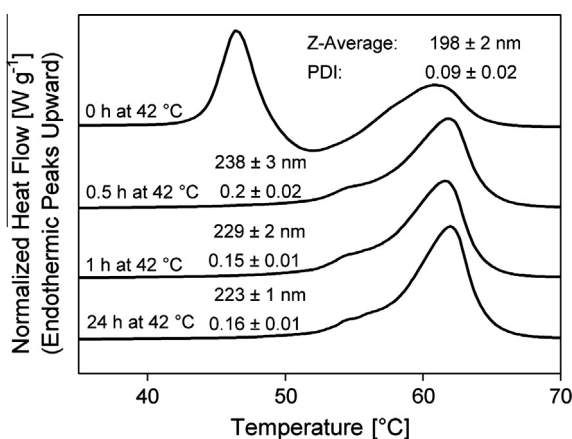


Fig. 12. DSC curves, PCS z-average and PDI values of a batch-crystallized S100-3/SGC-stabilized dispersion before and after thermal treatment at 42 °C. The corresponding PCS z-average and PDI values (measurements on two independent samples) are also given.

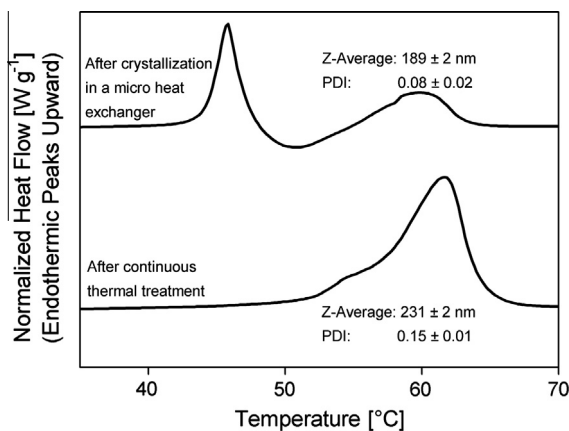


Fig. 13. DSC curves and z-average/PDI values of a S100-3/SGC-stabilized dispersion after continuous processing in a micro-heat exchanger and subsequent thermal treatment.

subsequent continuous thermal treatment of 1 h at 42 °C. It is obvious that continuous processing is possible leading to 100%  $\beta$ -modification for the S100-3/SGC-stabilized dispersion as expected based on the screening result.

#### 4. Conclusions

While the continuous crystallization of SLN offers significant advantages over batch processing, the desired stable  $\beta$ -modification may not be obtained in the crystallization step but needs additional thermal treatment. For favorable systems, an integrated continuous process sequence consisting of melt crystallization and subsequent thermal treatment can be established producing particle dispersions, which contain only the stable  $\beta$ -polymorph. A four step screening procedure has been investigated to identify and optimize suitable colloidal lipid dispersions: (i) characterization of the SLN dispersion concerning the melting points of involved crystal modifications, (ii) determination of the maximum temperature which can be used for a thermally induced polymorphic transformation into the stable  $\beta$ -modification without melting the existing metastable  $\alpha$ -form, (iii) evaluation of the  $\alpha$  to  $\beta$  transition kinetics, and (iv) final decision, if the continuous polymorphic transition to the stable crystal modification is possible in a defined timescale of 4 h. Once a lipid nanoparticle system suitable for continuous processing is identified, the screening plant can be used for standardized continuous melt crystallization and thermal treatment. With this method, it is possible to screen a wide range of different dispersions in order to identify and optimize promising formulations for the continuous melt crystallization in a micro-heat exchanger with subsequent thermal treatment for the purpose of producing stable products.

#### Acknowledgements

Financial support by the “Deutsche Forschungsgemeinschaft (DFG)” within the Research Group FOR 856 “Mikrosysteme für partikuläre Life-Science-Produkte (mikroPART)” is gratefully acknowledged. Furthermore, the authors thank Mrs. Handt (Technische Universität Braunschweig, Institut für Pharmazeutische Technologie, Germany) for the DSC measurements as well as Sasol Germany GmbH, Kuraray Specialities GmbH and Lipoid GmbH for providing raw materials.

#### Appendix A. Supplementary material

Supplementary data associated with this article can be found, in the online version, at <http://dx.doi.org/10.1016/j.ejpb.2013.08.009>.

#### References

- [1] T. Bayer, J. Jenck, M. Matlosz, *IMPULSE – Ein neuartiger Ansatz für die Prozessentwicklung*, Chem. Ing. Tech. 76 (2004) 528–533.
- [2] L. Grundemann, M. Schoenitz, S. Scholl, *Shorter time-to-market with micro-conti processes*, Chem. Ing. Tech. 84 (2012) 685–693.
- [3] E. Kolehmainen, I. Turunen, P. Oinas, *Intensified processes for continuous production of fine and specialty chemicals*, in: P. Jansens et al. (Eds.), Proc. of the Sustainable (Bio)Chemical Process Technology Incorporating the 6th Int. Conf. on Process Intensification, 2005, Delft.
- [4] P. Speiser, *Lipidnanopellets als Trägersystem für Arzneimittel zur peroralen Anwendung*, EP 0167825 A2 (1986).
- [5] M.R. Gasco, S. Morel, *Lipospheres from microemulsions*, Farmaco 45 (1990) 1127–1128.
- [6] B. Siekmann, K. Westesen, *Submicron-sized parenteral carrier systems based on solid lipids*, Pharm. Pharmacol. Lett. 1 (1992) 123–126.
- [7] R.H. Müller, W. Mehnert, J.-S. Lucks, C. Schwarz, A. zur Mühlen, H. Weyhers, C. Freitas, D. Rühl, *Solid lipid nanoparticles (SLN) – an alternative colloidal carrier system for controlled drug delivery*, Eur. J. Pharm. Biopharm. 41 (1995) 62–69.
- [8] R.H. Müller, M. Radtke, S.A. Wissing, *Solid lipid nanoparticles (SLN) and nanostructured lipid carriers (NLC) in cosmetic and dermatological preparations*, Adv. Drug Deliver. Rev. 54 (2002) 131–155.
- [9] H. Bunjes, B. Siekmann, *Manufacture, characterization and application of solid lipid nanoparticles as drug delivery systems*, in: S. Benita (Ed.), Microencapsulation, Marcel Dekker, New York, 2006, pp. 213–268.
- [10] D.J. McClements, Y. Li, *Structured emulsion-based delivery systems: controlling the digestion and release of lipophilic food components*, Adv. Colloid Interface Sci. 159 (2010) 213–228.
- [11] S. Chakraborty, D. Shukla, B. Mishra, S. Singh, *Lipid – an emerging platform for oral delivery of drugs with poor bioavailability*, Eur. J. Pharm. Biopharm. 73 (2009) 1–15.
- [12] H. Bunjes, *Lipid nanoparticles for the delivery of poorly water-soluble drugs*, J. Pharm. Pharmacol. 62 (2010) 1637–1645.
- [13] S. Joseph, H. Bunjes, *Solid lipid nanoparticles for drug delivery*, in: D. Douroumis, A. Fahr (Eds.), Drug Delivery Strategies for Poorly Water-soluble Drugs, John Wiley & Sons, Chichester, 2012, pp. 103–133.
- [14] R. Parhi, P. Suresh, *Preparation and characterization of solid lipid nanoparticles – a review*, Curr. Drug Discover. Technol. 9 (2012) 2–16.
- [15] W. Mehnert, K. Mäder, *Solid lipid nanoparticles: production, characterization and applications*, Adv. Drug Deliver. Rev. 47 (2001) 165–196.
- [16] T.S. Awad, T. Helgason, J. Weiss, E.A. Decker, D.J. McClements, *Effect of omega-3 fatty acids on crystallization, polymorphic transformation and stability of tripalmitin solid lipid nanoparticle suspensions*, Cryst. Growth Des. 9 (2009) 3405–3411.
- [17] T. Helgason, T.S. Awad, K. Kristbergsson, E.A. Decker, D.J. McClements, J. Weiss, *Impact of surfactant properties on oxidative stability of  $\beta$ -carotene encapsulated within solid lipid nanoparticles*, J. Agric. Food Chem. 57 (2009) 8033–8040.
- [18] R. Shukat, P. Relkin, *Lipid nanoparticles as vitamin matrix carriers in liquid food systems: on the role of high-pressure homogenisation, droplet size and adsorbed materials*, Colloids Surf., B 86 (2011) 119–124.
- [19] J.W. Hagemann, *Thermal behavior and polymorphism of acylglycerides*, in: N. Garti, K. Sato (Eds.), Crystallization and Polymorphism of Fats and Fatty Acids, Marcel Dekker Inc., New York, 1988, pp. 9–95.
- [20] C.E. Clarkson, T. Malkin, *Alternation in long-chain compounds. Part II. An X-ray and thermal investigation of the triglycerides*, J. Chem. Soc. 11 (1934) 666–671.
- [21] M. Kellens, H. Reynaers, *Study of the polymorphism of saturated monoacid triglycerides I: melting and crystallization behaviour of tristearin*, Fat Sci. Technol. 94 (1992) 94–100.
- [22] K. Sato, N. Garti, *Crystallization and polymorphic transformation: an introduction*, in: N. Garti, K. Sato (Eds.), Crystallization and Polymorphism of Fats and Fatty Acids, Marcel Dekker Inc., New York, 1988, pp. 3–7.
- [23] K. Westesen, H. Bunjes, M.H.J. Koch, *Physicochemical characterization of lipid nanoparticles and evaluation of their drug loading capacity and sustained release potential*, J. Control. Release 48 (1997) 223–236.
- [24] T. Helgason, T.S. Awad, K. Kristbergsson, D.J. McClements, J. Weiss, *Influence of polymorphic transformations on gelation of tripalmitin solid lipid nanoparticle suspensions*, J. Am. Oil Chem. Soc. 85 (2008) 501–511.
- [25] K. Jasch, N. Barth, S. Fehr, H. Bunjes, W. Augustin, S. Scholl, *A microfluidic approach for a continuous crystallization of drug carrier nanoparticles*, Chem. Eng. Technol. 32 (2009) 1806–1814.
- [26] K. Sato, T. Kuroda, *Kinetics of melt crystallization and transformation of tripalmitin polymorphs*, J. Am. Oil Chem. Soc. 64 (1987) 124–127.
- [27] B. Siekmann, K. Westesen, *Thermoanalysis of the recrystallization process of melt homogenized glyceride nanoparticles*, Colloids Surf., B: Biointerfaces 3 (1994) 159–175.
- [28] K. Westesen, M. Drechsler, H. Bunjes, *Colloidal dispersions based on solid lipids*, in: E. Dickinson, R. Miller (Eds.), Food Colloids: Fundamentals of Formulation, Royal Society of Chemistry, Cambridge, 2001, pp. 103–115.
- [29] H. Bunjes, M.H.J. Koch, K. Westesen, *Effect of particle size on colloidal solid triglycerides*, Langmuir 16 (2000) 5234–5241.
- [30] H. Bunjes, M.H. Koch, K. Westesen, *Influence of emulsifiers on the crystallization of solid lipid nanoparticles*, J. Pharm. Sci. 92 (2003) 1509–1520.
- [31] H. Bunjes, M.H. Koch, *Saturated phospholipids promote crystallization but slow down polymorphic transitions in triglyceride nanoparticles*, J. Control. Release 107 (2005) 229–243.
- [32] K.M. Rosenblatt, H. Bunjes, *Poly(vinyl alcohol) as emulsifier stabilizes solid triglyceride drug carrier nanoparticles in the  $\alpha$ -modification*, Mol. Pharm. 6 (2009) 105–120.
- [33] G. Schaal, *Untersuchungen einer Befilmungsmöglichkeit fester Arzneiformen mit modifizierten Triglycerid-Dispersionen*, Ph.D. Thesis, Jena, 2004.
- [34] H. Bunjes, K. Westesen, M.H. Koch, *Crystallization tendency and polymorphic transitions in triglyceride nanoparticles*, Int. J. Pharm. 129 (1996) 159–173.
- [35] H. Bunjes, F. Steiniger, W. Richter, *Visualizing the structure of triglyceride nanoparticles in different crystal modifications*, Langmuir 23 (2007) 4005–4011.